Histol Histopathol (2022) 37: 1185-1199

http://www.hh.um.es

Histology and Histopathology
From Cell Biology to Tissue Engineering

ORIGINAL ARTICLE **Open Access**

Hsa_circ_0048674 facilitates hepatocellular carcinoma progression and natural killer cell exhaustion depending on the regulation of miR-223-3p/PDL1

Suihui Li[1]*, Zhuangzhong Chen[1]*, Ruisheng Zhou[2]*, Sisi Wang[1], Wenping Wang[1], De Liu[3], Mengquan Li[3] and Tiansheng Guo[4]

[1]Tumor Center, First Affiliated Hospital of Guangzhou University of Traditional Chinese Medicine, [2]Institute of Tumor, [3]Clinical Medical College, Guangzhou University of Chinese Medicine and [4]Department of Oncology, Panyu Hospital of Chinese Medicine, Guangzhou, Guangdong, China

*Suihui Li, Zhuangzhong Chen and Ruisheng Zhou contributed equally to this work

Summary. Background. Circular RNAs (circRNAs) play vital regulatory roles in human cancers, including hepatocellular carcinoma (HCC). In this study, we aimed to explore the functions of hsa_circ_0048674 in HCC development.

Methods. Quantitative real-time polymerase chain reaction (qRT-PCR) assay was used to detect hsa_circ_0048674, ubiquitin-like with PHD and RING finger domains 1 (UHRF1), microRNA-223-3p (miR-223-3p) and programmed death ligand 1 (PDL1). RNase R assay and Actinomycin D assay were employed to analyze the stability of hsa_circ_0048674. Cell Counting Kit-8 (CCK-8) assay, colony formation assay and 5-ethynyl-2'- deoxyuridine (EdU) assay were conducted to assess cell proliferation. Flow cytometry analysis, transwell assay and tube formation assay were carried out for cell apoptosis, migration, invasion and angiogenesis, respectively. Western blot assay was adopted for protein levels. Dual-luciferase reporter assay and RNA immunoprecipitation (RIP) assay were used to analyze the relationship between miR-223-3p and hsa_circ_0048674 or PDL1. Murine xenograft model assay was conducted for the function of hsa_circ_0048674 *in vivo*. Immunohistochemistry (IHC) assay was used to detect Ki-67 level in tumor tissues. Enzyme linked immunosorbent assay (ELISA) kits were employed for the concentrations of inflammatory factors.

Results. Hsa_circ_0048674 was highly expressed in HCC tissues and cells. Silencing of hsa_circ_0048674 repressed cell growth, migration, invasion and angiogenesis and promoted apoptosis in HCC cells *in vitro* and hampered tumor growth *in vivo*. Hsa_circ_0048674 served as an miR-223-3p sponge to alter PDL1 expression. MiR-223-3p inhibition or PDL1 overexpression restored the impacts of hsa_circ_0048674 silencing on HCC malignant behaviors. In addition, hsa_circ_0048674 knockdown promoted natural killer (NK) cell-mediated cytotoxicity to HCC cells.

Conclusion. Hsa_circ_0048674 knockdown decelerated HCC progression through the mediation of the miR-223-3p/PDL1 axis.

Key words: HCC, hsa_circ_0048674, miR-223-3p, PDL1

Introduction

Hepatocellular carcinoma (HCC) is a highly refractory and globally prevalent cancer (Yang and Roberts, 2010; Hemming et al., 2016). The usual treatment options for HCC include chemotherapy, radiation therapy, liver transplantation and surgical resection, but metastasis and recurrence are still a challenge for HCC therapy (Oliveri et al., 2012; Intaraprasong et al., 2016). Despite new breakthroughs in diagnosis and therapy, the prognosis for advanced HCC remains poor (Dimitroulis et al., 2017; Siegel et al., 2019). Therefore, finding new therapeutic targets is crucial for improving the prognosis of HCC patients.

Circular RNAs (circRNAs) are a series of RNA transcripts produced by anti-splicing (Memczak et al., 2013; Chen, 2016). CircRNAs play important roles in multiple biological functions of different cancers (Zhang

Corresponding Author: Tiansheng Guo, Department of Oncology, Panyu Hospital of Chinese Medicine, No. 65 Qiaqiao East Road, Panyu District, Guangzhou City, Guangdong Province, 511400, PR China. e-mail: pyguots@163.com

DOI: 10.14670/HH-18-440

et al., 2018). Some circRNAs can function as competitive endogenous RNAs (ceRNAs) and influence the expression of genes linked to tumor genesis and development by interacting with microRNAs (miRNAs) (Qu et al., 2015). In HCC, circ_102166 was able to impede HCC growth and invasion by sponging miR-182/miR-184 (Li et al., 2021). Circ_HIPK3 aggravated the tumorigenesis of HCC via miR-582-3p-dependent regulation of DLX2 (Zhang et al., 2020a). Circ_0046599 promoted proliferation, metastasis and glycolysis by mediating miR-1258/RPN2 (Zhang et al., 2020a). Hsa_circ_0048674 (circRNA ubiquitin-like with PHD and RING finger domains 1, circUHRF1) was elevated in HCC (Zhang et al., 2020b). UHRF1 has been demonstrated to be a HCC-promoting gene in HCC and contributed to tumor cell progression (Liu et al., 2017; Ko et al., 2019). Even so, the functions of hsa_circ_0048674 in HCC remain largely unclear.

MiRNAs are short non-coding RNAs, playing crucial roles in the malignancy of cancers, including HCC (Li et al., 2020). Former studies have revealed the dual-roles of miR-223-3p in cancers. For instance, miR-223-3p acted as a tumor accelerator in gastric cancer (Ren et al., 2020), renal cell carcinoma (Zhang et al., 2020c) and lung cancer (Qin et al., 2020) and as an inhibitor in breast cancer (Zhao et al., 2021), papillary thyroid carcinoma (Liu et al., 2021) and colorectal cancer (Ma et al., 2020). In HCC, miR-223-3p blocked HCC cell growth and triggered apoptosis by NLRP3 (Wan et al., 2018). Moreover, circular RNA Interactome analysis showed that miR-223-3p shared hsa_circ_0048674 binding sites. However, the relation between hsa_circ_0048674 and miR-223-3p in HCC development is undefined.

In this work, the dysregulated expression of hsa_circ_0048674 was observed in HCC. Thus, we clarified the possible roles and related mechanisms of hsa_circ_0048674 in HCC development.

Materials and methods

Tissue acquisition and natural killer (NK) cells isolation

A total of 63 tumor tissues and adjacent non-tumor tissues were obtained from HCC patients at First Affiliated Hospital of Guangzhou University of Traditional Chinese Medicine. The proportion of NK cells was detected using flow cytometry. According to NK cell proportion in the blood, HCC patients were divided into 2 groups: ≤8% group (n=37) and >8% group (n=26).

The peripheral blood mononuclear cells (PBMCs) were acquired from 10 healthy donators through density gradient centrifugation. NK cells were obtained from PNMCs with the usage of human NK cell isolation kit (Shanghai Li Rui Biological Technology Co., Ltd., Shanghai, China).

Our research received approval from the Ethics Committee of First Affiliated Hospital of Guangzhou University of Traditional Chinese Medicine. The participants offered written informed consent. The clinicopathological characteristics of HCC patients are shown in Table 1.

Cell culture

THLE-2 cells were acquired from the American Type Culture Collection (ATCC, Manassas, VA, USA). HUVECs, Huh7 and HCCLM3 cells were acquired from Procell (Wuhan, China). All these cells were cultured in Dulbecco's modified Eagle's medium (DMEM; Procell) mixed with 10% fetal bovine serum (FBS; Procell) and 1% Penicillin-Streptomycin (Procell) in a humid incubator including 5% CO_2 at 37°C.

The isolated NK cells were maintained in RPMI1640 (Procell) added with 10% FBS (Procell), 2 mM L-glutamine (Sigma-Aldrich, St. Louis, MO, USA) and 100 U/mL IL-2 (Sigma-Aldrich) at an atmosphere of 5% CO_2 and 37°C.

Quantitative real-time polymerase chain reaction (qRT-PCR) assay

TRIzol (Invitrogen, Carlsbad, CA, USA) was applied to isolate RNA from tissues and cells. The generation of cDNAs was done through inverse

Table 1. Correlation between Clinical feature and hsa_circ_0048674 expression level in hepatocellular carcinoma patients.

Clinical feature		hsa_circ_0048674		
	n	High	Low	P -Value
Age		31	32	0.2588
≥60	30	17	13	
<60	33	14	19	
Gender				0.3002
Man	45	24	21	
Woman	18	7	11	
Tumor size				0.0320*
≥5cm	32	20	12	
<5cm	31	11	20	
Hepatitis				0.0825
Negative	40	23	17	
Positive	23	8	15	
TNM stage				0.0154*
III+IV	35	22	13	
I+II	28	9	19	
Lymph node metastasis				0.0107*
N0	41	25	16	
N1	22	6	16	
Distant metastasis				0.1448
M0	39	22	17	
M1	24	9	15	
Histological grade				0.5026
Well/ Moderate	38	20	18	
Poor	25	11	14	

*P<0.05

transcription by using Primer Script™ RT reagent (Takara, Dalian, China) or TaqMan MicroRNA Reverse Transcription reagent (Applied Biosystems, Foster City, CA, USA). QRT-PCR was conducted using SYBR Premix Ex Taq II (Takara). The data were computed by the $2^{-\Delta\Delta Ct}$ way with 18S rRNA and U6 snRNA used for normalization. The primers utilized in this research were: hsa_circ_0048674: (F: 5'-GGCCAGAGTGAGT CAGACAA-3' and R: 5'-AGGAGCTGGATGGTG TCATT-3'); UHRF1: (F: 5'-GCCATACCCTCTTC GACTACG-3' and R: 5'-GCCCCAATTCCGTCTC ATCC-3'); miR-223-3p: (F: 5'-TGTCAGTTTGTCAA ATACCCCA-3' and R: 5'-GCAGGGTCCGAGG TATTCG-3'); programmed death ligand 1 (PDL1): (F: 5'-GCTGCACTAATTGTCTATTGGGA-3' and R: 5'-AATTCGCTTGTAGTCGGCACC-3'); 18S rRNA: (F: 5'-GTGGTGTTGAGGAAAGCAGACA-3' and R: 5'-TGATCACACGTTCCACCTCATC-3'); U6: (F: 5'-GCTCGCTTCGGCAGCACATA-3' and R: 5'-ACGCTTCACGAATTTGCGT-3').

Subcellular fraction assay

Cytoplasmic and Nuclear RNA Purification Kit (Norgen Biotek, Thorold, Canada) was employed to segregate the nuclei and cytoplasm of Huh7 and HCCLM3 cells. QRT-PCR was conducted for hsa_circ_0048674 level with 18S rRNA or U6 acted as cytoplasmic transcript and nuclear transcript controls.

RNase R assay

The RNA in HCC cells was subjected to RNase R (Epicentre, Madison, WI, USA) for 15 min at 37°C. Next, the expression of hsa_circ_0048674 and UHRF1 was quantified with qRT-PCR.

Actinomycin D assay

To block transcription, Huh7 and HCCLM3 cells were exposed to actinomycin D (Sigma-Aldrich) for indicated times. The levels of hsa_circ_0048674 and UHRF1 mRNA were then examined.

Cell transfection

To silence hsa_circ_0048674 expression, hsa_circ_0048674 small interference RNA (si-hsa_circ_0048674) and hsa_circ_0048674 short hairpin RNA (sh-hsa_circ_0048674) were constructed, and si-NC and sh-NC were used as corresponding controls. Hsa_circ_0048674 overexpression vector was established to elevate hsa_circ_0048674 expression with circ-NC as a control. MiR-223-3p mimics (miR-223-3p) and miR-223-3p inhibitors (anti-miR-223-3p) were synthesized to increase or decrease miR-223-3p level with NC and anti-NC as controls. Si-PDL1 and PDL1 overexpression vector (PDL1) were used to reduce or elevate PDL1 expression with scramble and vector as controls. All the synthesis was finished by GenePharma (Shanghai, China) and transfected into cells utilizing Lipofectamine 2000 (Invitrogen).

Cell proliferation assay

HCC cell proliferation was evaluated by Cell Counting Kit-8 (CCK-8), Colony formation and 5-ethynyl-2'- deoxyuridine (EdU) assays.

For CCK-8 experiments, Huh7 and HCCLM3 cells in 96-well plates were incubated with CCK-8 (Sigma-Aldrich) for 2 h at indicated time points. The absorption (450 nm) was examined with a microplate reader (Bio-Rad, Hercules, CA, USA).

For colony formation examination, Huh7 and HCCLM3 cells with various transfections were added into 6-well plates and grown for 12 days. Next, the colonies were stained with crystal violet (Sigma-Aldrich), photographed and quantified.

For EdU assay, EdU incorporation assay (RiboBio, Guangzhou, China) was adopted. Briefly, the transfected Huh7 and HCCLM3 cells in 24-well plates were mixed with EdU for 2h. The cells were then immobilized using 4% paraformaldehyde (Sigma-Aldrich) and incubated with 0.3% Triton X-100. Subsequently, the cells were maintained with Aollo fluorescent staining solution and dyed with Hoechst 33342. The images were obtained with a fluorescence microscope (Olympus, Tokyo, Japan). The positive cell rate was computed.

Flow cytometry analysis

The transfected Huh7 and HCCLM3 cells suspended in binding buffer were dyed with Annexin V-fluorescein isothiocyanate (FITC; Vazyme, Nanjing, China) and propidium iodide (PI; Vazyme) in dark conditions. FACScan® flow cytometry (BD Biosciences, San Jose, CA, USA) was used to estimate cell apoptotic rate.

Transwell assay

The transwell chambers (BD Biosciences) pre-covered with (invasion) or without (migration) Matrigel (BD Biosciences) were used in this experiment. In short, the transfected Huh7 and HCCLM3 cells were pipetted into the upper chamber and the complete culture medium was added into the bottom chamber. Following cultivation for 24 h, the cells which passed through the membranes were stained with crystal violet (Sigma-Aldrich) and estimated at 100×magnification under a microscope (Olympus).

Tube formation assay

After the transfected Huh7 and HCCLM3 cells were cultured in DMEM (Procell) mixed with 10% FBS (Procell) for 6 h, the culture media were replaced with DMEM (Procell) mixed with 1% FBS (Procell) and cultured for a further 8 h. Then, the culture solution was

centrifuged to obtain the supernatant. 50 μL Matrigel (BD Biosciences) was added to the 24-well plates with incubation for 1 h at 37°C. Next, HUVECs were added into the top layer of Matrigel (BD Biosciences) and maintained with the supernatant for 12 h. The formation of blood vessel-like structures was observed and imaged with a microscope (Olympus).

Western blot assay

The protein was obtained with RIPA buffer (Sigma-Aldrich). 30 μg protein was resolved by sodium dodecyl sulfonate-polyacrylamide gel electrophoresis and blotted to polyvinylidene difluoride membranes (Millipore, Billerica, MA, USA). Then the membranes were mixed with 5% non-fat milk, maintained with primary antibodies against proliferating cell nuclear antigen (PCNA; bs-2006R; Bioss, Beijing, China), B-cell lymphoma-2 (Bcl-2, bs-33411R; Bioss), total-caspase 3(t-caspase 3; bs-0081R; Bioss), Cleaved-caspase 3 (C-caspase 3; bsm-33199M; Bioss), matrix metallopeptidase 2 (MMP2; bs-0412R; Bioss), MMP9 (bs-22502R; Bioss), PDL1 (bs-21778R; Bioss) or GAPDH (bs-2188R; Bioss) and probed with secondary antibody (bs-0295M-HRP; Bioss). The bands were visualized using the ECL kit (Vazyme).

Dual-luciferase reporter assay

Hsa_circ_0048674 or PDL1 3'UTR harboring the wild-type (wt) or mutant (mut) miR-223-3p binding sequences were introduced into pmirGLO vector (Promega, Fitchburg, WI, USA), generating hsa_circ_0048674-wt, hsa_circ_0048674-mut, PDL1-wt or PDL1 mut. Then, HCC cells were transfected with the vectors and miR-223-3p/NC. Dual-Luciferase Reporter Assay Kit (Promega) was used to examine the luciferase intensity.

RNA immunoprecipitation (RIP) assay

Huh7 and HCCLM3 cells were lysed utilizing RIP buffer which harbored Anti-IgG or Anti-Ago2-conjugated magnetic beads. After digestion with protease K (Solarbio, Beijing, China), the enrichment of hsa_circ_0048674, miR-223-3p and PDL1 was examined.

Murine xenograft model

Beijing Vital River Laboratory Animal Technology Co., Ltd. (Beijing, China) offered the BALB/c nude mice. The mice were allocated into 2 groups (N=7/group). Huh7 cells transfected with hsa_circ_0048674 shRNA lentiviral vectors (lenti-sh-hsa_circ_0048674) or lenti-sh-NC were introduced into the mice. Tumor volume was estimated every 5 days for 30 days via the formula: Length×Width^2/2. After 30 days, the mice were euthanized and tumor weight was examined. The experiment was permitted by the Ethics Committee of Animal Research of First Affiliated Hospital of Guangzhou University of Traditional Chinese Medicine.

Immunohistochemistry (IHC) assay

The xenograft tumor tissues were embedded in paraffin (Sigma-Aldrich) and sectioned. Then the sections were dewaxed, rehydrated and kept with anti-ki-67 (bs-2130R; Bioss), MMP2 (bs-4605R; Bioss) or MMP9 (bs-4593R; Bioss) at 4°C. On the second day, the sections were stained with a secondary streptavidin-HRP-conjugated antibody (Solarbio) and then treated with hematoxylin (Sigma-Aldrich).

Enzyme linked immunosorbent assay (ELISA)

The concentrations of interferon γ (IFN-γ) and tumor necrosis factor-α (TNF-α) were examined using related ELISA Kits (ab174443; ab181421; Abcam, Cambridge, MA, USA) according to the manufacturers' instructions.

Statistical analysis

GraphPad Prism 7 (GraphPad Inc., La Jolla, CA, USA) was adopted for data analysis. Each experiment was repeated three times. One-way analysis of variance and Student's t-test were employed for difference analysis. Spearman's correlation coefficient was adopted to analyze the relationship among the levels of hsa_circ_0048674, miR-223-3p and PDL1 mRNA in HCC tissues. $P<0.05$ was considered significant.

Results

Hsa_circ_0048674 was highly expressed in HCC tissues and cells

As exhibited in Fig. 1A, hsa_circ_0048674 (circUHRF1) was derived from the exon 3 of gene UHRF1 and the mature length was 255 nt. To explore the roles of hsa_circ_0048674 in HCC development, the expression level of hsa_circ_0048674 in HCC tissues and normal tissues was detected. It was found that hsa_circ_0048674 level was increased more than two folds in HCC tissues in comparison with normal tissues (Fig. 1B). Moreover, hsa_circ_0048674 level was related to tumor size, TNM stages and lymph node metastasis (Table 1). Then, we demonstrated that hsa_circ_0048674 was upregulated in Huh7 and HCCLM3 cells compared to THLE-2 cells (Fig. 1C). Moreover, subcellular fraction assay showed that hsa_circ_0048674 was mainly enriched in the cytoplasm of Huh7 and HCCLM3 cells (Fig. 1D). RNase R assay indicated that has_circ_0048674 could not be digested by RNase R, while UHRF1 was digested by RNase R (Fig. 1E). In addition, hsa_circ_0048674 possessed a longer half-life than linear UHRF1 (Fig. 1F). All these findings

indicated that hsa_circ_0048674 was stable and the aberrant expression of hsa_circ_0048674 might be associated with HCC development.

Hsa_circ_0048674 knockdown suppressed cell proliferation, migration, invasion and angiogenesis and promoted apoptosis in HCC cells

To explore the exact roles of hsa_circ_0048674 in HCC cell malignant behaviors, HCC cells with hsa_circ_0048674 knockdown were constructed by transfecting si-hsa_circ_0048674 into HCC cells. QRT-PCR assay presented that the expression of hsa_circ_0048674 was reduced in Huh7 and HCCLM3 cells transfected with si-hsa_circ_0048674 compared to si-NC groups (Fig. 2A). As illustrated by CCK-8 assay, hsa_circ_0048674 knockdown suppressed the viability of Huh7 and HCCLM3 cells compared to si-NC control groups (Fig. 2B). The results of colony formation assay showed that hsa_circ_0048674 silencing restrained the colony formation ability of Huh7 and HCCLM3 cells relative to control groups (Fig. 2C). EdU assay indicated that Huh7 and HCCLM3 cells with hsa_circ_0048674 silencing showed a marked suppression in cell proliferation (Fig. 2D). Flow cytometry analysis presented that hsa_circ_0048674 interference induced the apoptosis of Huh7 and HCCLM3 cells in comparison with control groups (Fig. 2E). Transwell assay showed that hsa_circ_0048674 knockdown inhibited the capacities of Huh7 and HCCLM3 cells to migrate and invade relative to control groups (Fig. 2F,G). Tube formation assay presented that the angiogenic ability of the HUVECs was inhibited by hsa_circ_0048674 silencing (Fig. 2H). Besides, the levels of proliferation-related protein (PCNA), apoptosis-related proteins (Bcl-2 and C-caspase 3/t-caspase 3) and metastasis-related proteins (MMP2 and MMP9) in si-hsa_circ_0048674 transfected HCC cells were measured via western blot assay. The results exhibited that hsa_circ_0048674 knockdown reduced the levels of PCNA, Bcl-2, MMP2 and MMP9 and elevated the level of C-caspase 3/t-caspase 3 in Huh7 and HCCLM3 cells (Fig. 2I). Taken together, hsa_circ_0048674 knockdown repressed the malignancy of HCC cells.

Hsa_circ_0048674 directly bound to miR-223-3p

Through analyzing circular RNA Interactome (https://circinteractome.nia.nih.gov/api/v2/mirnasearch?circular_rna_query=hsa_circ_0048674&mirna_query=hsa-miR-223&submit=miRNA+Target+Search), hsa_circ_0048674 was found to contain miR-223-3p binding sites (Fig. 3A). As illustrated by dual-luciferase

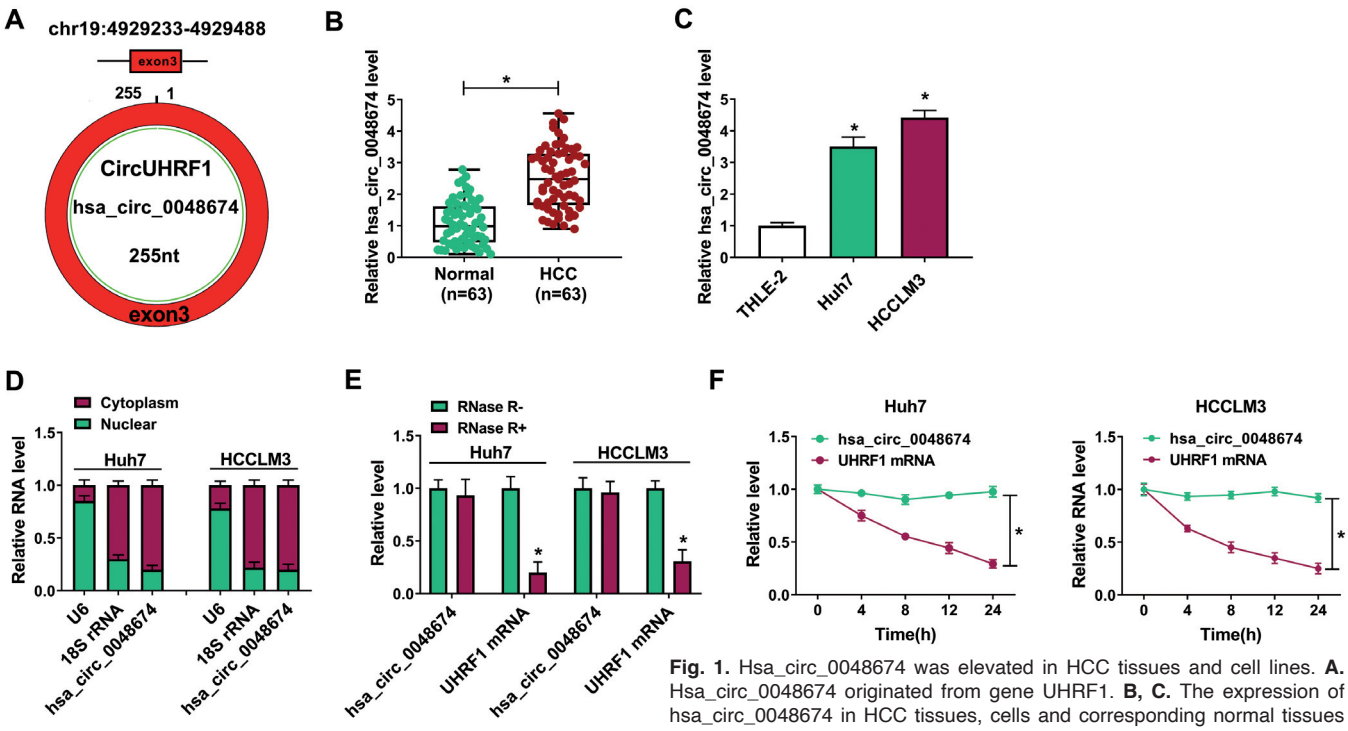

Fig. 1. Hsa_circ_0048674 was elevated in HCC tissues and cell lines. **A.** Hsa_circ_0048674 originated from gene UHRF1. **B, C.** The expression of hsa_circ_0048674 in HCC tissues, cells and corresponding normal tissues and cells was detected by qRT-PCR assay. **D.** The expression level of hsa_circ_0048674 in the cytoplasm and nuclei of Huh7 and HCCLM3 cells was analyzed. **E.** The levels of hsa_circ_0048674 and UHRF1 in Huh7 and HCCLM3 cells exposed to RNase R were determined by qRT-PCR assay. **F.** The half-life of hsa_circ_0048674 and UHRF1 was analyzed by actinomycin D assay. *P<0.05. The experiments were repeated three times.

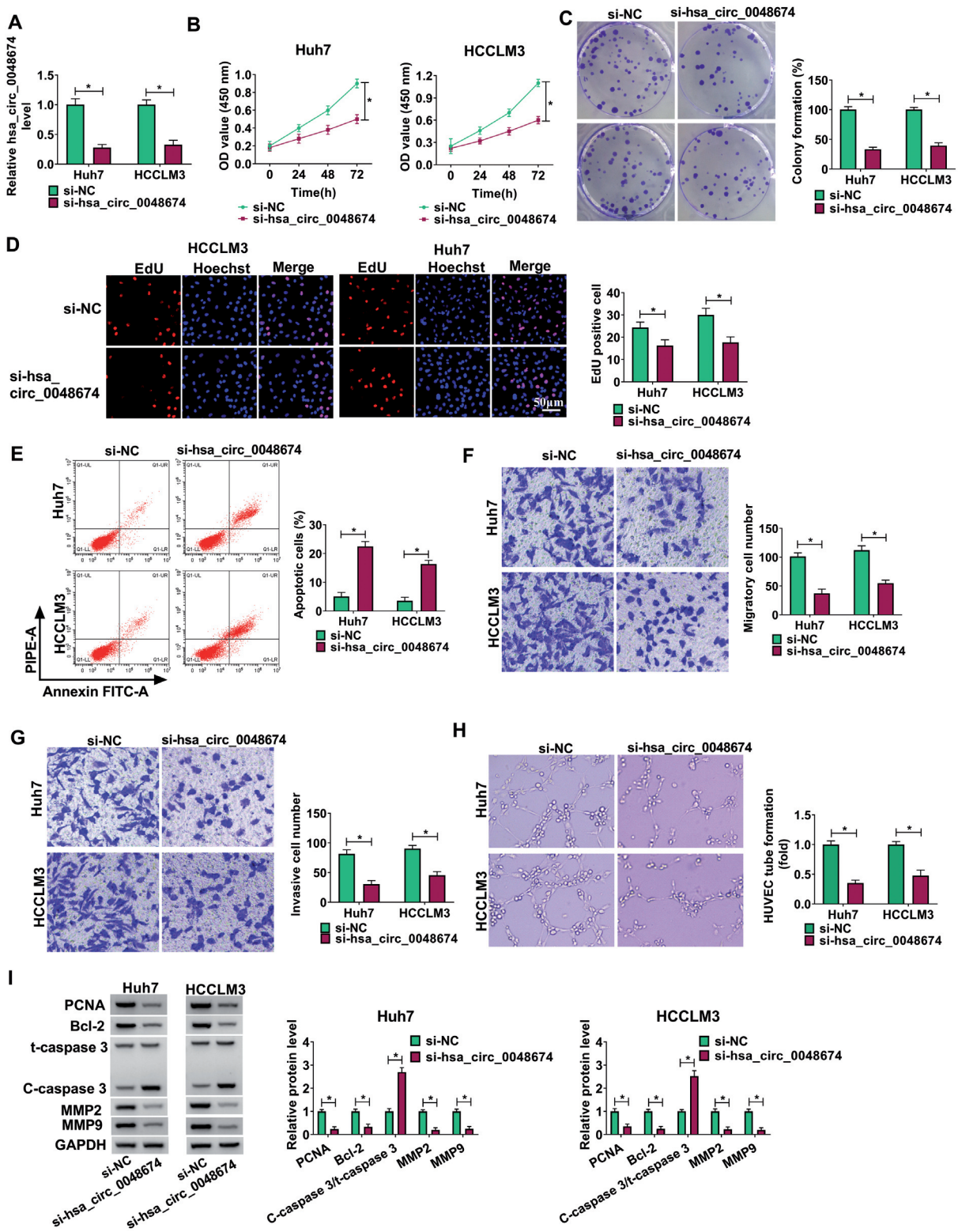

Fig. 2. Effects of hsa_circ_0048674 on HCC cell growth, apoptosis, migration, invasion and angiogenesis. **A.** The expression of hsa_circ_0048674 in Huh7 and HCCLM3 cells transfected with si-NC or si-hsa_circ_0048674 was detected by qRT-PCR assay. **B-D.** The proliferation ability of transfected Huh7 and HCCLM3 cells was assessed by CCK-8 assay, colony formation assay and EdU assay. **E.** The apoptosis of transfected Huh7 and HCCLM3 cells was analyzed by flow cytometry analysis. **F, G.** The migration and invasion of transfected Huh7 and HCCLM3 cells were evaluated by transwell assay. **H.** The angiogenesis capacity of transfected Huh7 and HCCLM3 cells was analyzed by tube formation assay. **I.** The protein levels of PCNA, Bcl-2, C-caspase 3/t-caspase 3, MMP2 and MMP9 in transfected Huh7 and HCCLM3 cells were measured by western blot assay. *P<0.05. The experiments were repeated three times.

reporter assay, the luciferase activity of hsa_circ_0048674-wt in Huh7 and HCCLM3 cells was reduced by miR-223-3p transfection, whereas the luciferase activity of hsa_circ_0048674-mut was not affected (Fig. 3B). RIP assay showed that hsa_circ_0048674 and miR-223-3p were markedly enriched in Anti-Ago2 immunoprecipitates compared to Anti-IgG groups (Fig. 3C). The transfection of hsa_circ_0048674 overexpression resulted in a remarkable increase in hsa_circ_0048674 expression in both Huh7 and HCCLM3 cells (Fig. 3D). Moreover, hsa_circ_0048674 overexpression reduced miR-223-3p expression, while hsa_circ_0048674 knockdown enhanced miR-223-3p expression in Huh7 and HCCLM3 cells (Fig. 3E). Indeed, in HCC tissues, miR-223-3p expression was decreased and inversely correlated with hsa_circ_0048674 expression (Fig. 3F,G). Besides, our results showed that miR-223-3p was lowly expressed in Huh7 and HCCLM3 cells compared to THLE-2 cells (Fig. 3H). Collectively, miR-223-3p was sponged by hsa_circ_0048674.

Hsa_circ_0048674 positively regulated PDL1 expression by decoying miR-223-3p

Subsequently, PDL1 was predicted to be a target gene of miR-223-3p through analyzing bioinformatics prediction software miRcode (http://www.mircode.org/?gene=CD274&mirfam=&class=&cons=&trregion=) (Fig. 4A). To verify the prediction, we then performed dual-luciferase reporter assay and RIP assay. Dual-luciferase reporter assay showed that miR-223-3p overexpression inhibited the luciferase activity of PDL1-wt, but did not affect the luciferase activity of PDL1-mut in Huh7 and HCCLM3 cells (Fig. 4B). RIP assay showed that miR-223-3p and PDL1 levels were elevated in Anti-Ago2 immunoprecipitates compared to Anti-IgG RIP groups, which further demonstrated the interaction between miR-223-3p and PDL1 (Fig. 4C). As presented in Fig. 4D, anti-miR-223-3p distinctly reduced miR-223-3p expression in Huh7 and HCCLM3 cells. Furthermore, we observed that hsa_circ_0048674 silencing downregulated PDL1 protein level in Huh7 and

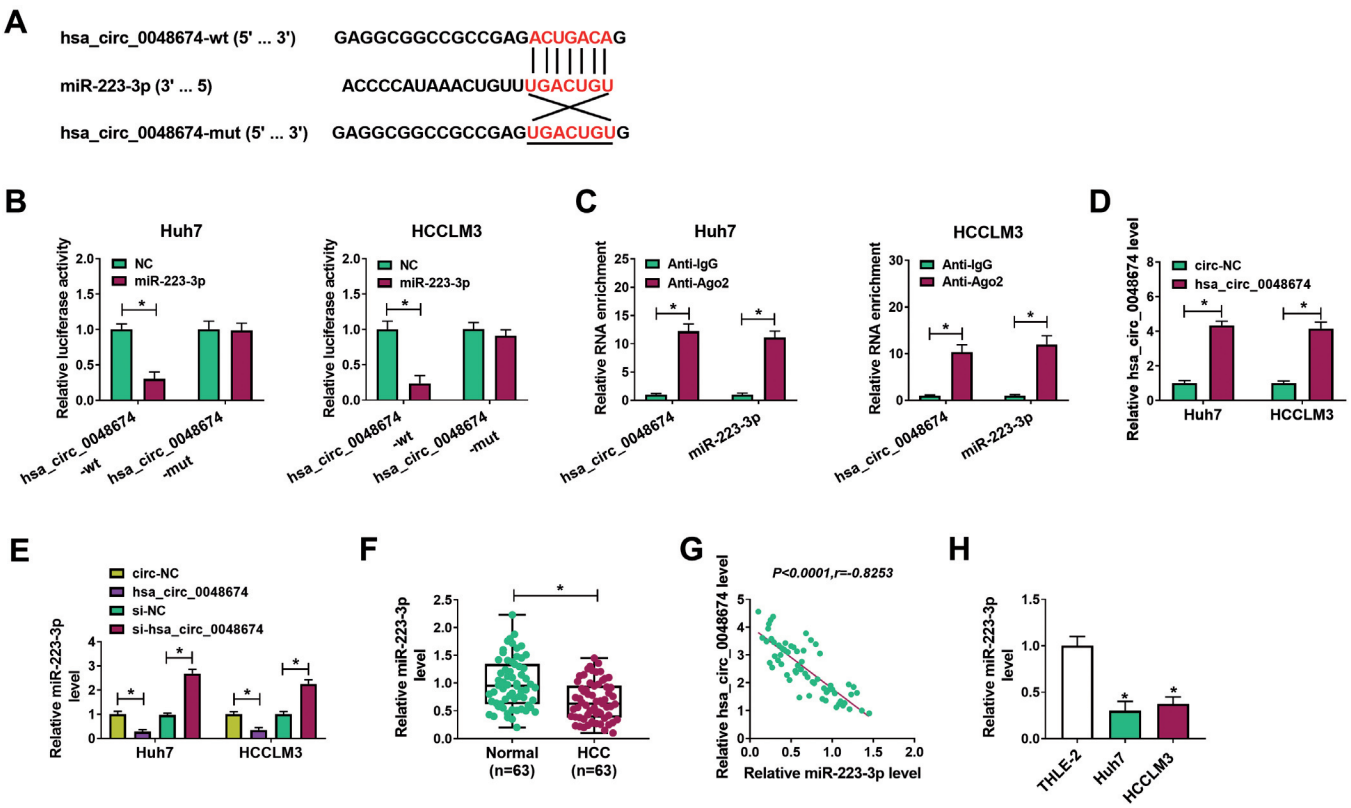

Fig. 3. Hsa_circ_0048674 directly targeted miR-223-3p. **A.** The binding sites between hsa_circ_0048674 and miR-223-3p. **B, C.** Dual-luciferase reporter assay and RIP assay adopted to analyze the relationship between hsa_circ_0048674 and miR-223-3p. **D.** The expression of hsa_circ_0048674 in circ-NC or hsa_circ_0048674 transfected Huh7 and HCCLM3 cells was detected by qRT-PCR assay. **E.** The expression of miR-223-3p in Huh7 and HCCLM3 cells transfected with circ-NC, hsa_circ_0048674, si-NC or si-hsa_circ_0048674 was detected using qRT-PCR assay. **F.** The expression of miR-223-3p in HCC tissues and normal tissues was examined by qRT-PCR assay. **G.** The linear correlation between the levels of hsa_circ_0048674 and miR-223-3p in HCC tissues was estimated. **H.** The expression of miR-223-3p in THLE-2, Huh7 and HCCLM3 cells was detected by qRT-PCR assay. *P<0.05. The experiments were repeated three times.

HCCLM3 cells, while miR-223-3p inhibition abated the impact (Fig. 4E). As expected, compared to normal tissues, PDL1 mRNA and protein levels in HCC tissues were enhanced (Fig. 4F,G). Of note, PDL1 mRNA level was positively correlated with hsa_circ_0048674 level and negatively correlated with miR-223-3p level in HCC tissues (Fig. 4H,I). In addition, the protein level of PDL1 was increased in Huh7 and HCCLM3 cells compared to THLE-2 cells (Fig. 4J). These findings suggested that hsa_circ_0048674 sponged miR-223-3p to alter PDL1

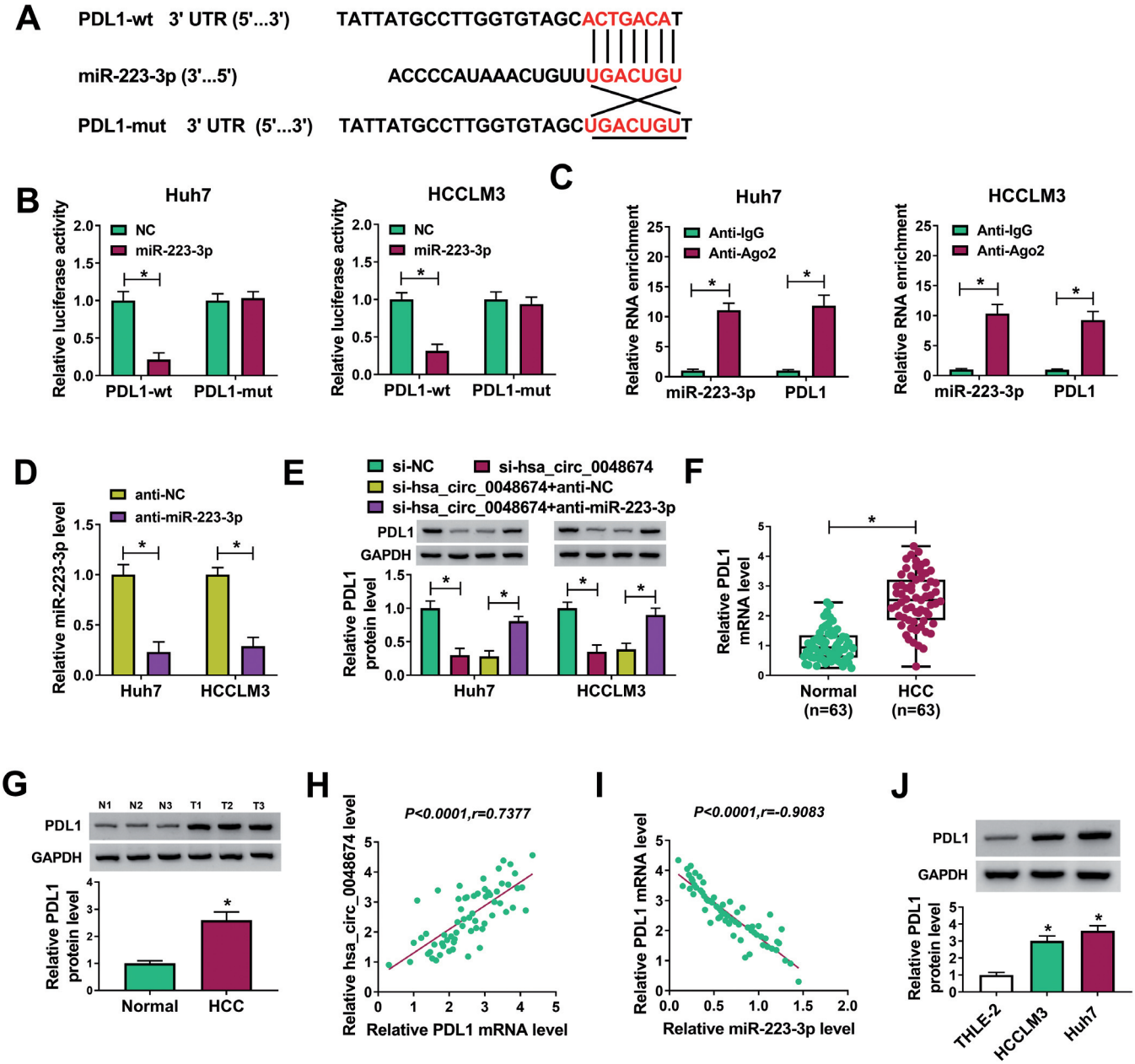

Fig. 4. PDL1 was the target gene of miR-223-3p. **A.** PDL1 contained the binding sites of miR-223-3p. **B, C.** The combination between miR-223-3p and PDL1 was estimated by dual-luciferase reporter assay and RIP assay. **D.** The expression of miR-223-3p in anti-NC or anti-miR-223-3p transfected Huh7 and HCCLM3 cells was detected by qRT-PCR assay. **E.** Following Huh7 and HCCLM3 cells were transfected with si-NC, si-hsa_circ_0048674, si-hsa_circ_0048674+anti-NC or si-hsa_circ_0048674+anti-miR-223-3p, PDL1 protein level was measured by western blot assay. **F, G.** The mRNA and protein of PDL1 in HCC tissues and normal tissues were examined by qRT-PCR assay or western blot assay. **H, I.** The correlation between the levels of PDL1 mRNA and hsa_circ_0048674/miR-223-3p was analyzed. **J.** The protein level of PDL1 in THLE-2, Huh7 and HCCLM3 cells was measured through western blot assay. *P<0.05. The experiments were repeated three times.

expression in HCC tissues.

PDL1 knockdown suppressed the malignant behaviors of HCC cells

To investigate the roles of PDL1 in HCC progression, si-PDL1 was transfected into Huh7 and HCCLM3 cells to knock down PDL1 expression. The transfection efficiency was examined by western blot assay, which showed that si-PDL1 transfection reduced PDL1 protein level in Huh7 and HCCLM3 cells (Fig. 5A). The results of CCK-8 assay, colony formation assay

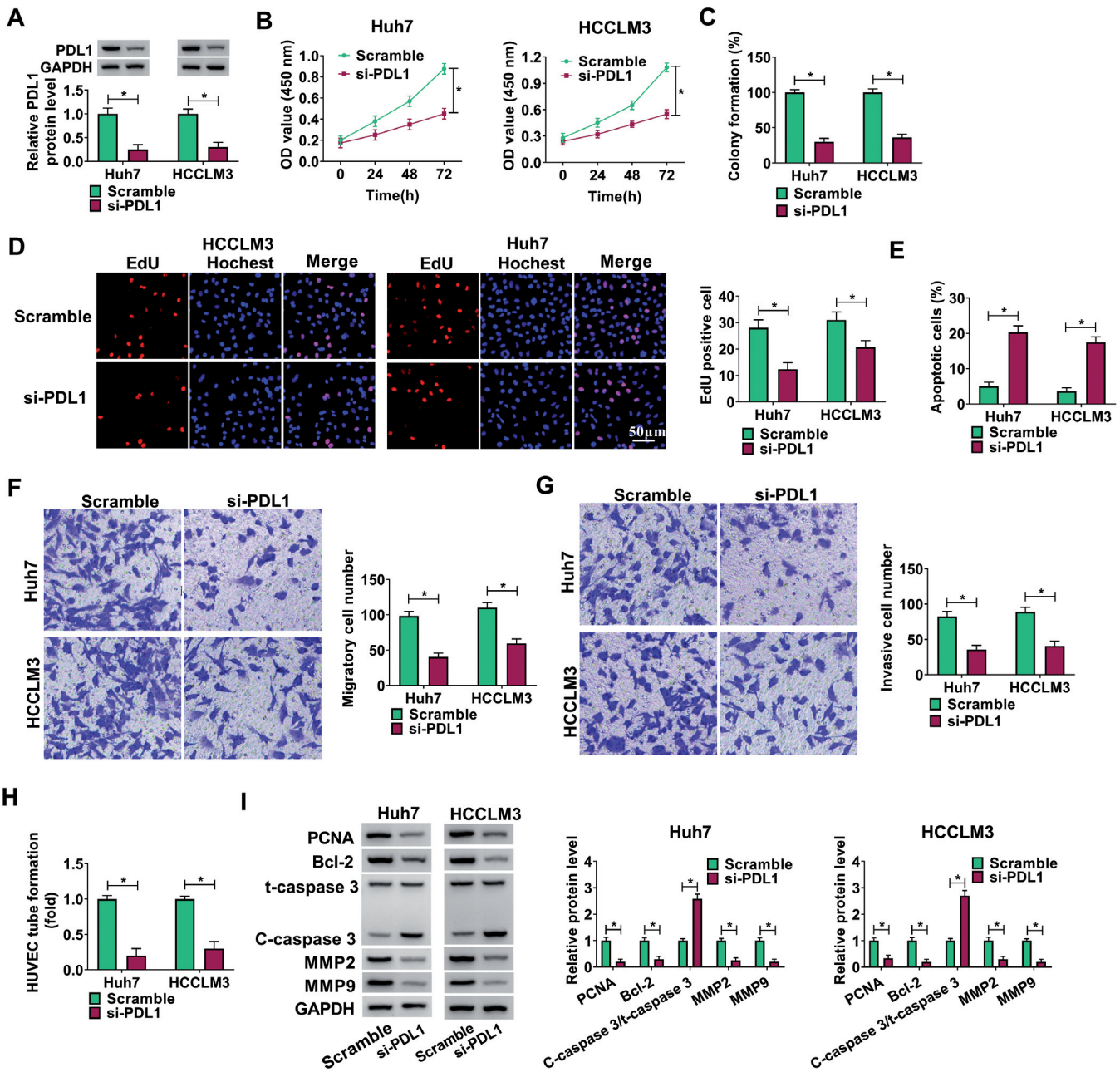

Fig. 5. Impacts of PDL1 silencing on HCC cell malignant phenotypes. Si-PDL1 or scramble was transfected into Huh7 and HCCLM3 cells. **A.** The protein level of PDL1 in Huh7 and HCCLM3 cells was measured via western blot assay. **B-D.** The proliferation of Huh7 and HCCLM3 cells was assessed by CCK-8 assay, colony formation assay and EdU assay. **E.** The apoptosis of Huh7 and HCCLM3 cells was analyzed by flow cytometry analysis. **F, G.** The migration and invasion of Huh7 and HCCLM3 cells were tested by transwell assay. **H.** The tube formation ability of HUVECs was analyzed via tube formation assay. **I.** The protein levels of PCNA, Bcl-2, C-caspase 3/t-caspase 3, MMP2 and MMP9 in Huh7 and HCCLM3 cells were measured via western blot assay. *P<0.05. The experiments were repeated three times.

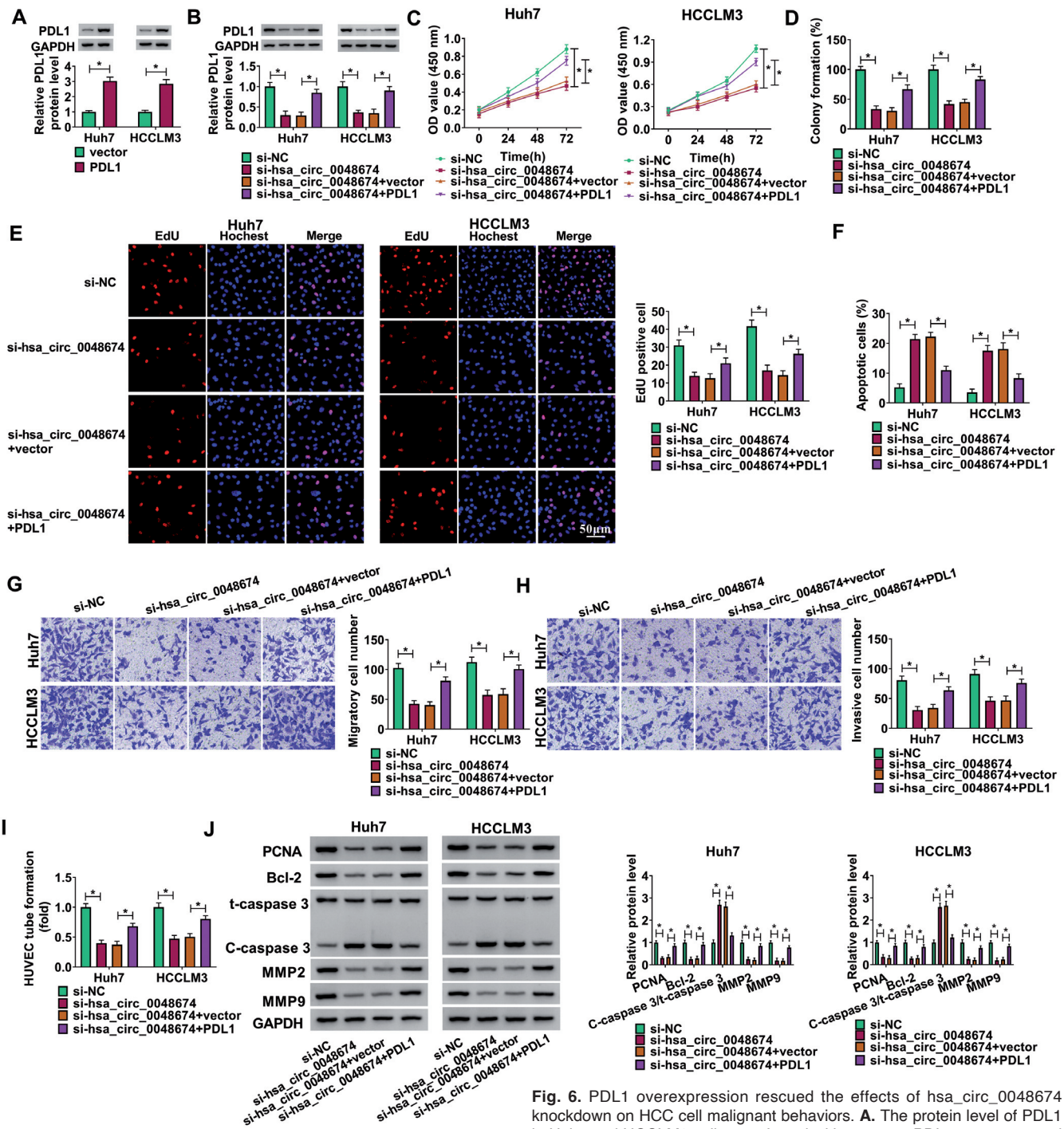

Fig. 6. PDL1 overexpression rescued the effects of hsa_circ_0048674 knockdown on HCC cell malignant behaviors. **A.** The protein level of PDL1 in Huh7 and HCCLM3 cells transfected with vector or PDL1 was measured by western blot assay. **B-J.** Huh7 and HCCLM3 cells were transfected with si-NC, si-hsa_circ_0048674, si-hsa_circ_0048674+vector or si-hsa_circ_0048674+PDL1. **B.** The protein level of PDL1 in Huh7 and HCCLM3 cells was measured using western blot assay. **C-E.** The proliferation of Huh7 and HCCLM3 cells was assessed by CCK-8 assay, colony formation assay and EdU assay. **F.** The apoptosis of Huh7 and HCCLM3 cells was analyzed by flow cytometry analysis. **G, H.** The migration and invasion of Huh7 and HCCLM3 cells were evaluated by transwell assay. **I.** The angiogenesis ability of HUVECs was analyzed by tube formation assay. **J.** The protein levels of PCNA, Bcl-2, C-caspase 3/t-caspase 3, MMP2 and MMP9 in Huh7 and HCCLM3 cells were measured using western blot assay. *P<0.05. The experiments were repeated three times.

and EdU assay indicated that PDL1 silencing apparently restrained the capacity of Huh7 and HCCLM3 cells to proliferate compared to scramble control groups (Fig. 5B-D). PDL1 deficiency promoted Huh7 and HCCLM3 cell apoptosis relative to scramble control groups (Fig. 5E). Transwell assay indicated that PDL1 knockdown repressed the migration and invasion of Huh7 and HCCLM3 cells relative to control groups (Fig. 5F,G). Moreover, tube formation assay exhibited that PDL1 silencing inhibited the tube formation ability of HUVECs in comparison with control groups (Fig. 5H). In addition, PDL1 interference decreased the levels of PCNA, Bcl-2, MMP2 and MMP9 and increased C-caspase 3/t-caspase 3 in Huh7 and HCCLM3 cells (Fig. 5I). These outcomes suggested that PDL1 knockdown suppressed HCC cell progression.

PDL1 overexpression reversed the effects of hsa_circ_0048674 knockdown on cell proliferation, apoptosis, migration, invasion and angiogenesis

As shown in Fig. 6A, PDL1 protein level was increased in Huh7 and HCCLM3 cells after PDL1 overexpression vector transfection. To elucidate the relationship between hsa_circ-0048674 and PDL1 in HCC progression, Huh7 and HCCLM3 cells were transfected with si-NC, si-hsa_circ_0048674, si-hsa_circ_0048674+vector or si-hsa_circ_0048674+PDL1. Western blot assay showed that hsa_circ_0048674 silencing reduced PDL1 protein level in Huh7 and HCCLM3 cells, while PDL1 overexpression reversed the effect (Fig. 6B). The suppressive role of hsa_circ_0048674 in the proliferation of Huh7 and HCCLM3 cells was ameliorated by elevating PDL1 expression (Fig. 6C-E). Flow cytometry analysis indicated the promotional effect of hsa_circ_0048674 silencing on Huh7 and HCCLM3 cell apoptosis was abolished by PDL1 overexpression (Fig. 6F). Transwell assay exhibited that hsa_circ_0048674 knockdown repressed the migration and invasion of Huh7 and HCCLM3 cells, whereas PDL1 upregulation overturned the impacts (Fig. 6G,H). As demonstrated by tube formation assay, PDL1 overexpression promoted the hsa_circ_0048674 knockdown-mediated angiogenesis ability of HUVECs (Fig. 6I). Moreover, PDL1 enhancement ameliorated the effects of hsa_circ_0048674 deficiency on the protein levels of PCNA, Bcl-2, C-caspase 3/t-caspase 3, MMP2 and

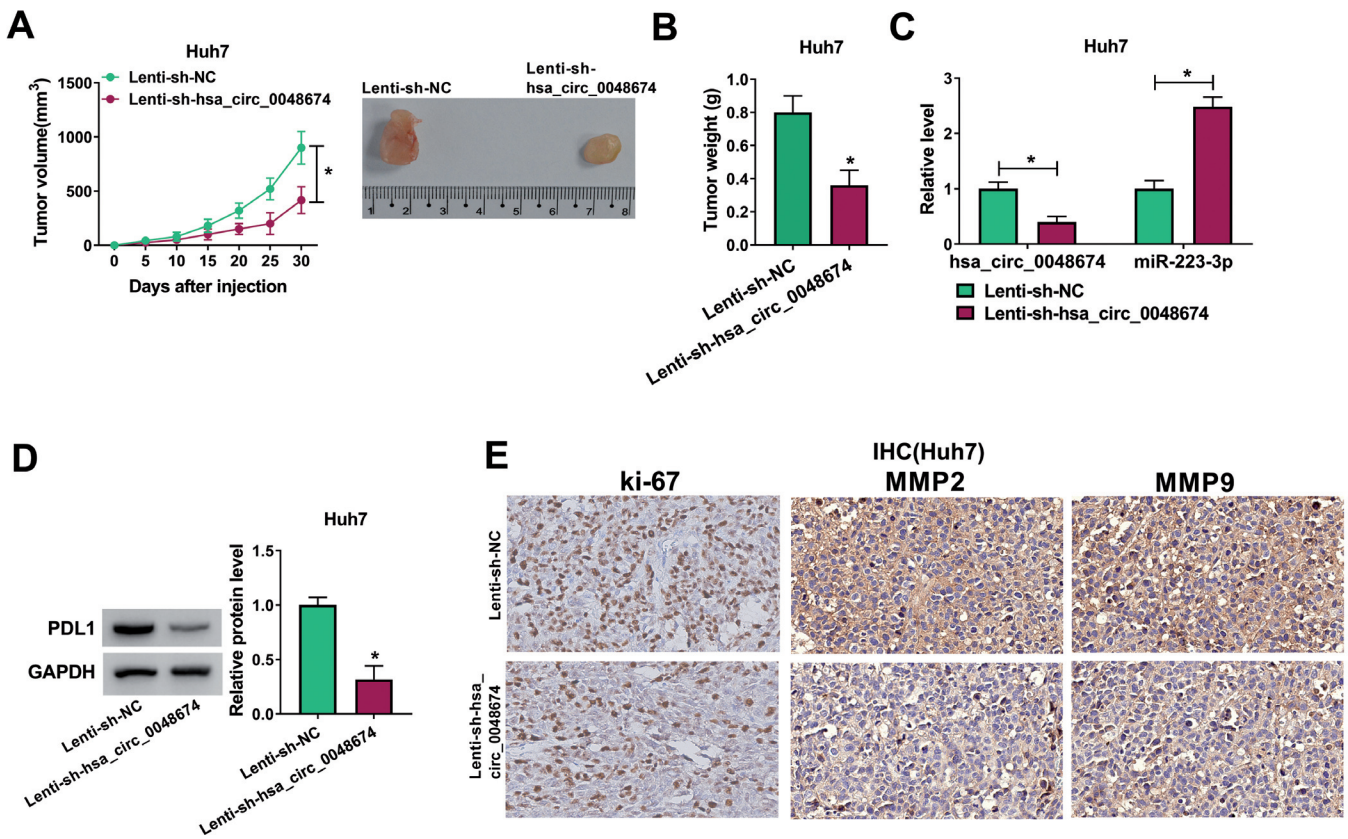

Fig. 7. Hsa_circ_0048674 knockdown blocked tumorigenesis *in vivo*. **A, B.** Tumor volume and tumor weight were measured. **C.** The levels of hsa_circ_0048674 and miR-223-3p in the xenograft tumors were detected by qRT-PCR assay. **D.** The protein level of PDL1 in the xenograft tumors was measured by western blot assay. **E.** The levels of ki-67, MMP2 and MMP9 were estimated by IHC assay. *P<0.05. The experiments were repeated three times.

MMP9 in Huh7 and HCCLM3 cells (Fig. 6J). To summarize, hsa_circ_0048674 knockdown restrained the malignant behaviors of HCC cells by upregulating PDL1 expression.

Hsa_circ_0048674 knockdown suppressed tumor growth in vivo

To explore the functional role of hsa_circ_0048674 in tumor formation *in vivo*, the murine xenograft model was established. Our results showed that the mice with hsa_circ_0048674 knockdown possessed reduced tumor volume and tumor weight compared to control groups (Fig. 7A,B). Moreover, we found that hsa_circ_0048674 and PDL1 protein level were decreased and miR-223-3p level was increased in the xenograft tumors in Lenti-sh-has_circ_0048674 groups compared to Lenti-sh-NC control groups (Fig. 7C,D). IHC assay showed that ki-67, MMP2 and MMP9 levels were reduced in the xenograft tumors with has_circ_0048674 silencing compared to control groups (Fig. 7E). The results indicated that hsa_circ_0048674 knockdown hampered tumor growth *in vivo*.

Hsa_circ_0048674 knockdown promoted the functions of NK cells

According to NK cell proportion in the blood, HCC patients were divided into 2 groups: ≤ 8% group (n=37) and > 8% group (n=26). QRT-PCR assay showed that hsa_circ_0048674 level was reduced in NK cell proportion > 8% group compared to ≤ 8% group (Fig. 8A). Next, to explore whether hsa_circ_0048674 could regulate NK cells, NK cells were cultured with Huh7 cells or HCCLM3 cells for 24 h. Compared to culture without Huh7 or HCCLM3 cell groups, NK cells cultured with Huh7 or HCCLM3 cells showed a reduction in IFN-γ and TNF-α concentrations when subsequently cultured with K562 cells (Fig. 8B). Moreover, the level of hsa_circ_0048674 was increased in NK cells cultured with Huh7 or HCCLM3 cells compared to NK cells cultured alone (Fig. 8C). To further explore whether the effects of HCC cells on NK cells were mediated by hsa_circ_0048674, Huh7 and HCCLM3 cells were transfected with si-hsa_circ_0048674 to knock down hsa_circ_0048674 expression. Of note, we found that hsa_circ_0048674

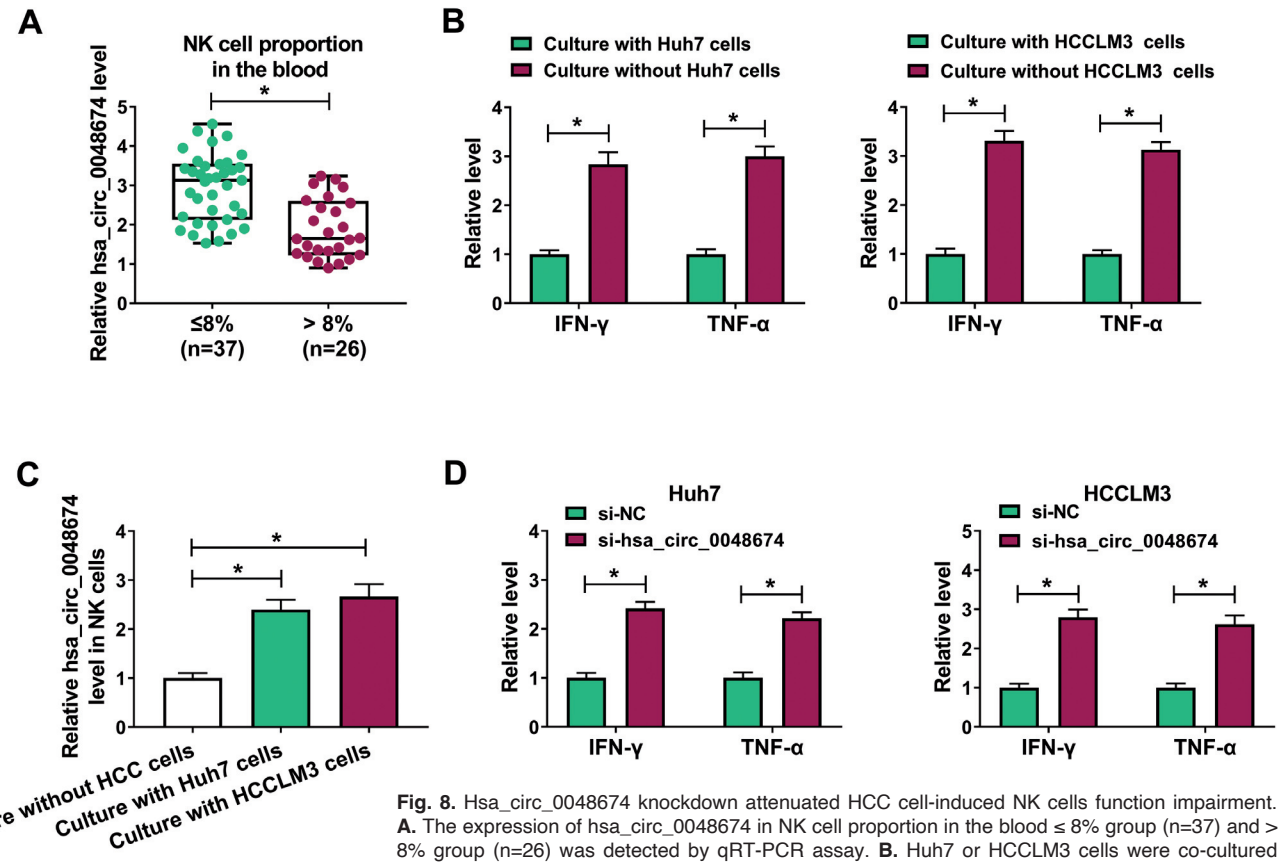

Fig. 8. Hsa_circ_0048674 knockdown attenuated HCC cell-induced NK cells function impairment. **A.** The expression of hsa_circ_0048674 in NK cell proportion in the blood ≤ 8% group (n=37) and > 8% group (n=26) was detected by qRT-PCR assay. **B.** Huh7 or HCCLM3 cells were co-cultured with NK cells at a 1:1 ratio for 24 h and then NK cells were co-cultured with K562 cells for 72 h followed by detection of IFN-γ and TNF-α concentrations. **C.** The expression of hsa_circ_0048674 in NK cells co-cultured with or without Huh7 or HCCLM3 cells was detected by qRT-PCR assay. **D.** The levels of IFN-γ and TNF-α in HK cells co-cultured with si-NC or si-hsa_circ_0048674 transfected Huh7 or HCCLM3 cells were examined with ELISA kits. *P<0.05. The experiments were repeated three times.

knockdown recovered HCC cell-induced impairment of IFN-γ and TNF-α concentrations in NK cells (Fig. 8D). Taken together, hsa_circ_0048674 inhibited the functions of NK cells.

Discussion

In recent years, circRNAs have been noted to play essential regulatory functions in the occurrence of cancers, including HCC (Lin and Chen, 2018). Nonetheless, the roles of most circRNAs in HCC remain undefined. In this project, the aberrant elevation of hsa_circ_0048674 promoted the development of HCC. Moreover, a hsa_circ_0048674/miR-223-3p/PDL1 network was discovered in HCC.

In HCC, the functional regulation of circRNAs has been gradually validated. For example, circ_0001178 (Gao et al., 2020), circPVT1 (Zhu et al., 2019), hsa_circ_0061395 (Yu et al., 2021) were able to decrease tumor cell proliferation and motility and trigger apoptosis in HCC. Moreover, hsa_circ_0002185 (circUHRF1) aggravated the carcinogenesis of oral squamous cell carcinoma (Zhao et al., 2020) and hsa_circ_0048677 (circUHRF1) induced NK cell exhaustion in HCC (Zhang et al., 2020b). Hsa_circ_0048674 also originates from UHRF1, but its functions in HCC are still unclear. In this study, hsa_circ_0048674 was detected to be upregulated in HCC tissues and cell lines. Hsa_circ_0048674 silencing restrained HCC cell proliferation, migration and invasion *in vitro*, concomitant with downregulation of PCNA, Bcl-2, MMP2 and MMP9 and upregulation of C-caspase 3/t-caspase 3. It is documented that the angiogenesis of solid tumors is a predominant event associated with tumor growth and metastasis (Hernández-Romero et al., 2019). Moreover, circRNAs are involved in the progression of cancers by regulating angiogenesis (Hernandez-Romero et al., 2019). For instance, circASH2L facilitated the tumorigenesis and angiogenesis of ovarian cancer by impacting miR-665/VEGFA (Chen et al., 2020). Circ_001587/miR-223/SLC4A4 repressed the angiogenesis and metastasis of pancreatic cancer (Zhang et al., 2020d). Herein, the impact of hsa_circ_0048674 on angiogenesis in HCC was explored. It was found that hsa_circ_0048674 downregulation inhibited the angiogenesis ability of HCC. Additionally, murine xenograft tumor formation was blocked after hsa_circ_0048674 silencing. All these findings indicated the oncogenic properties of hsa_circ_0048674 in HCC.

Subsequently, we discovered that miR-223-3p was sponged by hsa_circ_0048674. Zhang et al. suggested that miR-223-3p repressed HCC malignancy by regulating IGF-1R (Zhang and Zhang, 2018). Wan et al. claimed that miR-223-3p overexpression induced HCC cell apoptosis and restrained proliferation by binding to NLRP3 (Wan et al., 2018). Here, miR-223-3p was lowly expressed in HCC. Moreover, hsa_circ_0048674 knockdown promoted miR-223-3p level in HCC cells. However, we did not investigate the precise roles of miR-223-3p in HCC.

PDL1 is an immune-associated protein and plays a vital role in inhibiting tumor immunity and promoting tumor progression after combining with PD-1 (Topalian et al., 2012). PDL1 can induce the apoptosis of activated tumor-reactive T cells, leading to local immune suppression of T cells, thereby facilitating tumor growth and metastasis (Dong et al., 2002). In addition, PDL1 played a vital role in a variety of tumors cells independently from effects on immune cells (Passariello et al., 2019). For example, PDL1 elevation is linked to tumor aggressiveness and recurrence in HCC via resulting tumor cell progression (Gao et al., 2009; Mocan et al., 2019). PDL1 can be targeted by miR-34a (Huang et al., 2017), miR-200a (Wei et al., 2019) and miR-320a (Costa et al., 2020) to participate in cancer progression. Herein, PDL1 was identified to be targeted by hsa_circ_0048674 for the first time. Furthermore, we demonstrated that PDL1 interference curbed cell growth, motility and angiogenesis and enhanced apoptosis in HCC cells. PDL1 overexpression restored the impacts of hsa_circ_0048674 deficiency on HCC cell malignant biological phenotypes.

NK cells are immune modulation cells for tumor immunity and NK cell immunodeficiency is correlated with the occurrence of malignant tumors (Taketomi et al., 1998; Shimasaki et al., 2020). Currently, several circRNAs have been found to affect the susceptibility of HCC cells to NK cells. For example, hsa_circ_0007456 overexpression enhanced the cytotoxicity of NK cells to HCC via miR-6852-3p/ICAM-1 (Shi et al., 2021). NK cells showed enhanced cytotoxicity against HCC cells by circARSP91 elevation (Ma et al., 2019). Moreover, exosomal circUHRF1 was able to induce NK cell exhaustion depending on miR-449c-5p/TIM-3 (Zhang et al., 2020b). In this work, we found that hsa_circ_0048674 silencing promoted NK cell functions in HCC cells, but whether hsa_circ_0048674 could influence NK cell cytotoxicity was still unclear.

Taken together, the hsa_circ_0048674/miR-223-3p/PDL1 axis had an oncogenic effect on HCC through promoting tumor cell growth, migration, invasion and angiogenesis and inhibiting apoptosis. Our findings might afford a novel method for HCC treatment.

Acknowledgements. Not applicable.

Ethics approval and consent to participate. The present study was approved by the ethical review committee of First Affiliated Hospital of Guangzhou University of Traditional Chinese Medicine with approval No. 20210215. Written informed consent was obtained from all enrolled patients.

Consent for publication. Patients agree to participate in this work

Availability of data and materials. The analyzed data sets generated during the present study are available from the corresponding author on reasonable request.

Competing interests. The authors declare that they have no competing interests.

Funding. No funding was received.

References

Chen J., Li X., Yang L., Li M., Zhang Y. and Zhang J. (2020). CircASH2L promotes ovarian cancer tumorigenesis, angiogenesis, and lymphangiogenesis by regulating the miR-665/VEGFA axis as a competing endogenous RNA. Front. Cell Dev. Biol. 8, 595585.

Chen L.L. (2016). The biogenesis and emerging roles of circular RNAs. Nat. Rev. Mol. Cell Biol. 17, 205-211.

Costa C., Indovina P., Mattioli E., Forte I.M., Iannuzzi C.A., Luzzi L., Bellan C., De Summa S., Bucci E., Di Marzo D., De Feo M., Mutti L., Pentimalli F. and Giordano A. (2020). P53-regulated miR-320a targets PDL1 and is downregulated in malignant mesothelioma. Cell Death Dis. 11, 748.

Dimitroulis D., Damaskos C., Valsami S., Davakis S., Garmpis N., Spartalis E., Athanasiou A., Moris D., Sakellariou, S., Kykalos S., Tsourouflis G., Garmpi A., Delladetsima I., Kontzoglou K. and Kouraklis G. (2017). From diagnosis to treatment of hepatocellular carcinoma: An epidemic problem for both developed and developing world. World J. Gastroenterol. 23, 5282-5294.

Dong H., Strome S.E., Salomao D.R., Tamura H., Hirano F., Flies D.B., Roche P.C., Lu J., Zhu G., Tamada K., Lennon V.A., Celis E. and Chen L. (2002). Tumor-associated B7-H1 promotes T-cell apoptosis: a potential mechanism of immune evasion. Nat. Med. 8, 793-800.

Gao Q., Wang X.Y., Qiu S.J., Yamato I., Sho M., Nakajima Y., Zhou J., Li B.Z., Shi Y.H., Xiao Y.S., Xu Y. and Fan J. (2009). Overexpression of PD-L1 significantly associates with tumor aggressiveness and postoperative recurrence in human hepatocellular carcinoma. Clin. Cancer Res. 15, 971-979.

Gao S., Hu W., Huang X., Huang X., Chen W., Hao L., Chen Z., Wang J. and Wei H. (2020). Circ_0001178 regulates miR-382/VEGFA axis to facilitate hepatocellular carcinoma progression. Cell Signal. 72, 109621.

Hemming A.W., Berumen J. and Mekeel K. (2016). Hepatitis B and hepatocellular carcinoma. Clin. Liver Dis. 20, 703-720.

Hernandez-Romero I.A., Guerra-Calderas L., Salgado-Albarran M., Maldonado-Huerta T. and Soto-Reyes E. (2019). The regulatory roles of non-coding RNAs in angiogenesis and neovascularization from an epigenetic perspective. Front. Oncol. 9, 1091.

Huang X., Xie X., Wang H., Xiao X., Yang L., Tian Z., Guo X., Zhang L., Tang H. and Xie X. (2017). PDL1 and LDHA act as ceRNAs in triple negative breast cancer by regulating miR-34a. J. Exp. Clin. Cancer Res. 36, 129.

Intaraprasong P., Siramolpiwat S. and Vilaichone R.K. (2016). Advances in management of hepatocellular carcinoma. Asian Pac. J. Cancer Prev. 17, 3697-3703.

Ko E., Kim J.S., Bae J.W., Kim J., Park S.G. and Jung G. (2019). SERPINA3 is a key modulator of HNRNP-K transcriptional activity against oxidative stress in HCC. Redox Biol. 24, 101217.

Li D., Zhang J. and Li J. (2020). Role of miRNA sponges in hepatocellular carcinoma. Clin. Chim. Acta 500, 10-19.

Li R., Deng Y., Liang J., Hu Z., Li X., Liu H., Wang G., Fu B., Zhang T., Zhang Q., Yang Y., Chen G. and Liu W. (2021). Circular RNA circ-102166 acts as a sponge of miR-182 and miR-184 to suppress hepatocellular carcinoma proliferation and invasion. Cell Oncol. (Dordr). 44, 279-295.

Lin X. and Chen Y. (2018). Identification of potentially functional CircRNA-miRNA-mRNA regulatory network in hepatocellular carcinoma by integrated microarray analysis. Med. Sci. Monit Basic Res. 24, 70-78.

Liu X., Ou H., Xiang L., Li X., Huang Y. and Yang D. (2017). Elevated UHRF1 expression contributes to poor prognosis by promoting cell proliferation and metastasis in hepatocellular carcinoma. Oncotarget 8, 10510-10522.

Liu Y., Zhang H., Wang H., Du J., Dong P., Liu M. and Lin Y. (2021). Long non-coding RNA DUXAP8 promotes the cell proliferation, migration, and invasion of papillary thyroid carcinoma via miR-223-3p mediated regulation of CXCR4. Bioengineered 12, 496-506.

Ma Y., Zhang C., Zhang B., Yu H. and Yu Q. (2019). circRNA of AR-suppressed PABPC1 91 bp enhances the cytotoxicity of natural killer cells against hepatocellular carcinoma via upregulating UL16 binding protein 1. Oncol. Lett. 17, 388-397.

Ma Y.L., Wang C.Y., Guan Y.J. and Gao F.M. (2020). Long noncoding RNA ROR promotes proliferation and invasion of colorectal cancer by inhibiting tumor suppressor gene NF2 through interacting with miR-223-3p. Eur. Rev. Med. Pharmacol. Sci. 24, 2401-2411.

Memczak S., Jens M., Elefsinioti A., Torti F., Krueger J., Rybak A., Maier L., Mackowiak S.D., Gregersen L.H., Munschauer M., Loewer A., Ziebold U., Landthaler M., Kocks C., le Noble F. and Rajewsky N. (2013). Circular RNAs are a large class of animal RNAs with regulatory potency. Nature 495, 333-338.

Mocan T., Sparchez Z., Craciun R., Bora C.N. and Leucuta D.C. (2019). Programmed cell death protein-1 (PD-1)/programmed death-ligand-1 (PD-L1) axis in hepatocellular carcinoma: prognostic and therapeutic perspectives. Clin. Transl. Oncol. 21, 702-712.

Oliveri R.S., Wetterslev J. and Gluud C. (2012). Hepatocellular carcinoma. Lancet 380, 470; author reply 470-471.

Passariello M., D'Alise A.M., Esposito A., Vetrei C., Froechlich G., Scarselli E., Nicosia A. and De Lorenzo C. (2019). Novel human anti-PD-L1 mabs inhibit immune-independent tumor cell growth and PD-L1 associated intracellular signalling. Sci. Rep. 9, 13125.

Qin L., Zhong M., Adah D., Qin L., Chen X., Ma C., Fu Q., Zhu X., Li Z., Wang N. and Chen Y. (2020). A novel tumour suppressor lncRNA F630028O10Rik inhibits lung cancer angiogenesis by regulating miR-223-3p. J. Cell Mol. Med. 24, 3549-3559.

Qu S., Yang X., Li X., Wang J., Gao Y., Shang R., Sun W., Dou K. and Li H. (2015). Circular RNA: A new star of noncoding RNAs. Cancer Lett. 365, 141-148.

Ren N., Jiang T., Wang C., Xie S., Xing Y., Piao D., Zhang T. and Zhu Y. (2020). LncRNA ADAMTS9-AS2 inhibits gastric cancer (GC) development and sensitizes chemoresistant GC cells to cisplatin by regulating miR-223-3p/NLRP3 axis. Aging (Albany NY) 12, 11025-11041.

Shi M., Li Z.Y., Zhang L.M., Wu X.Y., Xiang S.H., Wang Y.G. and Zhang Y.Q. (2021). Hsa_circ_0007456 regulates the natural killer cell-mediated cytotoxicity toward hepatocellular carcinoma via the miR-6852-3p/ICAM-1 axis. Cell Death Dis. 12, 94.

Shimasaki N., Jain A. and Campana D. (2020). NK cells for cancer immunotherapy. Nat. Rev. Drug Discov. 19, 200-218.

Siegel R.L., Miller K.D. and Jemal A. (2019). Cancer statistics, 2019. CA Cancer J. Clin. 69, 7-34.

Taketomi A., Shimada M., Shirabe K., Kajiyama K., Gion T. and Sugimachi K. (1998). Natural killer cell activity in patients with hepatocellular carcinoma: a new prognostic indicator after hepatectomy. Cancer 83, 58-63.

Topalian S.L., Drake C.G. and Pardoll D.M. (2012). Targeting the PD-1/B7-H1(PD-L1) pathway to activate anti-tumor immunity. Curr. Opin. Immunol. 24, 207-212.

Wan L., Yuan X., Liu M. and Xue B. (2018). miRNA-223-3p regulates

NLRP3 to promote apoptosis and inhibit proliferation of hep3B cells. Exp. Ther. Med. 15, 2429-2435.

Wei S., Wang K., Huang X., Zhao Z. and Zhao Z. (2019). LncRNA MALAT1 contributes to non-small cell lung cancer progression via modulating miR-200a-3p/programmed death-ligand 1 axis. Int. J. Immunopathol. Pharmacol. 33, 2058738419859699.

Yang J.D. and Roberts L.R. (2010). Hepatocellular carcinoma: A global view. Nat. Rev. Gastroenterol. Hepatol. 7, 448-458.

Yu Y., Bian L., Liu R., Wang Y. and Xiao X. (2021). Circular RNA hsa_circ_0061395 accelerates hepatocellular carcinoma progression via regulation of the miR-877-5p/PIK3R3 axis. Cancer Cell Int. 21, 10.

Zhang C. and Zhang J. (2018). Decreased expression of microRNA-223 promotes cell proliferation in hepatocellular carcinoma cells via the insulin-like growth factor-1 signaling pathway. Exp. Ther. Med. 15, 4325-4331.

Zhang H.D., Jiang L.H., Sun D.W., Hou J.C. and Ji Z.L. (2018). CircRNA: a novel type of biomarker for cancer. Breast Cancer 25, 1-7.

Zhang H., Dai Q., Zheng L., Yuan X., Pan S. and Deng J. (2020a). Knockdown of circ_HIPK3 inhibits tumorigenesis of hepatocellular carcinoma via the miR-582-3p/DLX2 axis. Biochem. Biophys. Res. Commun. 533, 501-509.

Zhang P.F., Gao C., Huang X.Y., Lu J.C., Guo X.J., Shi G.M., Cai J.B. and Ke A.W. (2020b). Cancer cell-derived exosomal circUHRF1 induces natural killer cell exhaustion and may cause resistance to anti-PD1 therapy in hepatocellular carcinoma. Mol. Cancer 19, 110.

Zhang R.L., Aimudula A., Dai J.H. and Bao Y.X. (2020c). RASA1 inhibits the progression of renal cell carcinoma by decreasing the expression of miR-223-3p and promoting the expression of FBXW7. Biosci. Rep. 40.

Zhang X., Tan P., Zhuang Y. and Du L. (2020d). hsa_circRNA_001587 upregulates SLC4A4 expression to inhibit migration, invasion, and angiogenesis of pancreatic cancer cells via binding to microRNA-223. Am. J. Physiol. Gastrointest Liver Physiol. 319, G703-G717.

Zhao W., Cui Y., Liu L., Qi X., Liu J., Ma S., Hu X., Zhang Z., Wang Y., Li H., Wang Z., Liu Z. and Wu J. (2020). Splicing factor derived circular RNA circUHRF1 accelerates oral squamous cell carcinoma tumorigenesis via feedback loop. Cell Death Differ. 27, 919-933.

Zhao Y., Zhong R., Deng C. and Zhou Z. (2021). Circle RNA circABCB10 modulates PFN2 to promote breast cancer progression, as well as aggravate radioresistance through facilitating glycolytic metabolism via miR-223-3p. Cancer Biother. Radiopharm. 36, 477-490.

Zhu Y., Liu Y., Xiao B., Cai H., Liu M., Ma L., Yin H. and Wang F. (2019). The circular RNA PVT1/miR-203/HOXD3 pathway promotes the progression of human hepatocellular carcinoma. Biol. Open 8, bio043687.

Accepted February 21, 2022